IEEE Access
Multidisciplinary | Rapid Review | Open Access Journal

Received 12 May 2024, accepted 16 June 2024, date of publication 21 June 2024, date of current version 28 June 2024.

Digital Object Identifier 10.1109/ACCESS.2024.3417445

RESEARCH ARTICLE

An Enhanced Activated Zeroing Neural Dynamics for Solving Complex Matrix Inverse and Tracking Trajectory of Robotic Manipulator

JIALIANG CHEN[1], YIHUI LEI[2], AND BOLIN LIAO[1]
[1]College of Computer Science and Engineering, Jishou University, Jishou 416000, China
[2]College of Mathematics and Statistics, Jishou University, Jishou 416000, China

Corresponding author: Bolin Liao (mulinliao8184@163.com)

This work was supported in part by the National Natural Science Foundation of China under Grant 62066015, and in part by the Natural Science Foundation of Hunan Province of China under Grant 2023JJ30485.

ABSTRACT As an important branch of recurrent neural dynamics (RND), zeroing neural dynamics (ZND) can effectively deal with the dynamic complex matrix inverse (DCMI) issues. The convergence and robustness are two key performance indicators of the neuromotor system. For simultaneously realizing faster convergence rate and good noise-tolerance, some variant ZND models combined nonlinear activation function (NL-AF) and modified evolution formula are proposed. Though the performance of these ZND models is improved, the computational burden is sharply increased and some efficiency is lost. Furthermore, existing NL-AFs accelerate the convergence speed but still cannot satisfy the need of rigid time constraint. As we know, many classical NL-AFs have been put forward, few of them synthetically refer to achieving fixed time convergence and robust. Therefore, this work constructs a modified nonlinearly-activated ZND (MNAZND) model by implanting a novel versatile activation function (NV-AF) for solving the noise disturbed DCMI, the designed NV-AF includes the original term, the linear term and the discontinuous term, the original term ensures fixed time convergence, the linear and the discontinuous terms suppress different dynamic noises. Furthermore, with different noise state, the fixed-time convergence upper bound of the MNAZND model is deduced in theoretical proof. The numerical experiment verifies the MNAZND model with the proposed NV-AF has better fixed-time convergence and noise tolerance, the convergence time is less than theoretical fixed time $1/(\sigma\tau_1)$, and comparative simulation results also demonstrate that the designed NV-AF are advantageous over the previous AFs. Finally, the designed MNAZND is applied to tracking trajectory of robotic manipulator, which further illustrates reliability of the MNAZND.

INDEX TERMS Zeroing neural dynamics, nonlinear activation function, fixed-time convergence, robust, dynamic complex matrix inverse.

I. INTRODUCTION

As an essential step in many solution, matrix inverse problems arise frequently in mathematical and engineering applications, such as pattern recognition [1], metamaterial absorbers [2], machine learning [3], robots [4], [5], probability measures [6], UAVs control [7] etc. Due to the essential role of matrix inverse, lots of numerical iteration algorithms have been used to solve matrix inverse [8], [9], [10], [11], [12], [13]. For instance, in [9], a QR decomposition algorithm for solving matrix inverse was presented and applied to MIMO systems. Stanimirović et. al developed some matrix inverses algorithms which are applicable to real and complex matrix [10]. Leithead and Zhang proposed an iteration algorithm based on quasi-Newton BFGS method gain on the inverse of covariance matrix [12]. As we know, these presented algorithms with sequential processing property are inherently designed for static matrix inverse. When these iteration algorithms are applied to solving dynamic matrix inverse, it has been proven that the time complexity of complete the solving task is proportional to n^3 (n denotes the size of matrix). It means that the computational complexity

The associate editor coordinating the review of this manuscript and approving it for publication was Hassen Ouakad.

will rapidly increase, if these algorithms are used to dealing with high-order dynamic matrix. That means the calculation task will fail.

Over the last two decades, RND has received considerable research and has made great progress in theory and application. So RND has become the most powerful alternative for online calculations [14], [15], [16], [17], [18]. Especially, gradient-based RND (GND) and its extensions were proposed for handling matrix inverse [19], [20], [21]. However, on account of neglecting the velocity compensation of time-varying coefficients, the solution of GND always lags behind the theoretical solution when GND is used to solve dynamic computing problem. In order to eliminate the lag error in solving dynamic computing problem (including dynamic matrix inverse). Zhang and Sam Ge formally presented zeroing neural dynamics (ZND) [22]. The core design of ZND is constructing a derivative evolution formula, which can perfectly trace dynamic solution by employing the time derivative of time-varying parameters. Therefore, the dynamic lag error of ZND reduces to zero with the time goes. This is a huge leap forward in the field of RND. Since then, ZND and its extensions have been widely applied and gotten great success in the real domain [5], [23], [24], [25], [26], [27], [28], [29].

It is well known that the complex dynamic problems frequently occur in some fields, such as electronics, informatics, social systems, etc [30], [31]. In contrast to the ZND models defined in the real domain, the complex ZND models have shown competitive advantage in pattern recognition, signal and image processing [32], [33], [34]. To ensure the stability and global convergence of the complex ZND, usually only linear activation function (L-AF) is utilized. Actually, nonlinearly activated ZND (NAZND) model implanted well-designed nonlinear activation function will demonstrate superior performances. To improve convergence speed, the researchers exploited some special nonlinear activation functions (NL-AFs). For example, the bipolar-sigmoid activation function (BS-AF), power activation function (P-AF), power-sum activation function (PS-AF), hyperbolic sine activation function (HS-AF) and smooth power-sigmoid activation function (SPS-AF) were often be employed to accelerate the convergent speed in the early phase [23]. Compared with the ZND model activated by L-AF, the one activated by aforementioned NL-AFs significantly improved the convergent rate. However, it still takes a long time to converge to the exact solution. Under this background, efforts were further made to explore more specific activation functions to achieve finite time convergence. In [35], a sign-bi-power activation function (SBP-AF) was designed and studied in ZND models. It is heartening to note that the ZND model embedded the SBP-AF has superior finite time convergence. Moreover, an optimized SBP-AF (OSBP-AF) is proposed, which has more concise structure and also endows ZND better finite time convergence [36], [37], [38]. Nevertheless, according to theoretical demonstrations and simulation results, these finite-time convergent speed decided by NL-AFs (including SBP-AF and OSBP-AF) is closely related to the initial error of the corresponding ZND model, which can't satisfy the application need in hard time constraint states. On the other hand, all kinds of external noise will inevitably appear during ZND model online processing, which reduces the convergence speed and deteriorates the accuracy. To enhance the anti-noise capacity of ZND model, some improved evolution formulas were presented [5], [39], [40]. In [5], an integral evolution formula is introduced in ZND model for reducing the sensitivity to noises. Xiao et.al proposed a time-varying parameter ZND model, the design of time-varying parameter guarantees that the ZND model owns noise suppression capability [39]. However, the convergence effect of ZND model with improved evolution formula is not so good, and activation functions still be embedded in the improved formulas to enhanced convergence, which increases computational burden and brings efficiency loss.

As suggested above, this work constructs a modified nonlinearly-activated ZND (MNAZND) model by implanting a novel versatile activation function (NV-AF) for solving the noise disturbed dynamic complex matrix inverse (DCMI). the proposed NV-AF includes the original term, the linear term and the discontinuous term, thereinto, the design of the discontinuous term is inspired in slid mode noise control. The NV-AF makes the MNAZND model have both fixed-time convergence (i.e. the convergence time can be inferred in advance) and noise tolerance. It means that the MNAZND model can not only converge to exact analytical solution in a explicitly definite time but also can tolerate bounded dynamic vanishing noise, non-vanishing noise et al. In contrast to the existing ZND models, the MNAZND model improves the convergence and noise tolerance simultaneously only by implanting an ingenious complex-valued NL-AF, which conveniently enhances the online processing capability of the ZND. This is a remarkable improvement on the complex NAZND models, such a fixed-time and noise-tolerant MNAZND model in complex domain has not been mentioned in literature. Moreover, in view of exponential form is more concise and convenient in dealing with complex mathematical problems, a novel exponent nonlinear activation type is adopted in this paper. For better readability, all the abbreviations and corresponding full titles are listed in Table 1.

II. MODEL DESCRIPTION

In this section, we describe the MNAZND model for solving the CDMI. Firstly, the DCMI is introduced as:

$$Z(t)\Phi(t) = I, \text{ or } \Phi(t)Z(t) = I, \tag{1}$$

where $\Phi(t) \in C^{n\times n}$ denotes a known nonsingular time-varying matrix, I is the identity matrix of the same order as $\Phi(t)$, $Z(t)$ denotes the complex square matrix to be solved.

TABLE 1. The abbreviations and corresponding full titles.

Abbreviation	Full title	Abbreviation	Full title
DCMI	dynamic complex matrix inverse	NAZND	nonlinearly activated ZND
RND	recurrent neural dynamics	GND	gradient-based RND
ZND	zeroing neural dynamics	MNAZND	modified nonlinearly-activated ZND
L-AF	linear activation function	NL-AF	nonlinear activation function
P-AF	power activation function	PS-AF	power-sum activation function
BS-AF	bipolar-sigmoid activation function	SPS-AF	smooth power-sigmoid activation function
SBP-AF	sign-bi-power activation function	OSBP-AF	optimized SBP-AF
HS-AF	hyperbolic sine activation function	NV-AF	novel versatile activation function

According to the design process of ZND model in [35], an error function $\mathfrak{D}(t) = \Phi(t)Z(t) - I$ is defined to trace and optimize the solving process of ZND for dealing with the DCMI. The core design of ZND is a proportion derivative controller, and the evolution formula is

$$\dot{\mathfrak{D}}(t) = -\sigma\mathfrak{D}(t).$$

Literatures [35], [36], and [37] revealed that NL-AF prompts the ZND achieving finite-time convergence, therefore, the evolution formula activated by nonlinear function is given as

$$\dot{\mathfrak{D}}(t) = -\sigma\mathfrak{A}(\mathfrak{D}(t)), \tag{2}$$

where $\mathfrak{A}(\cdot)$ represents a complex-valued activation type, the definition of the complex-valued activation type $\mathfrak{A}(\cdot)$ is given as:

$$\mathfrak{A}(P + iQ) = \mathbb{J}(\tau) \circ \exp(i\Theta), \tag{3}$$

where $P + iQ$ is a complex number, τ and Θ respectively indicates the modulus and the argument of $P + iQ$, and $\mathbb{J}(\cdot)$ denotes a NL-AF. Though NL-AF can significantly improve the convergence of ZND, poorly designed activation function may lead to chattering in ZND implementation. To facilitate online processing, as revealed by simulations in [33], [35], and [37], the following NL-AF: PS-AF, HS-AF, SBP-AF and OSBP-AF were frequently employed to raise convergence speed. However, all of these activation functions have weak noise suppression ability. To overcome this defect, this paper proposes a NV-AF to ensure a fixed time convergence and a stronger noise suppression performance, $\mathbb{J}(\cdot)$ is designed as:

$$\mathbb{J}(e) = (\tau_1 \exp(|e|^k)|e|^{1-k}/k + \tau_2)\text{sign}(e) + \tau_3 e, \tag{4}$$

where the parameters $0 < k < 1, \tau_1 > 0, \tau_2, \tau_3 \geq 0$, and $\text{sign}(\cdot)$ is the signum function. $\mathbb{J}(\cdot)$ consists of three terms, $\tau_1 \exp(|e|^k)|e|^{1-k}\text{sign}(e)/k$ is the original term, which is to ensure fixed time convergence, $\tau_3 e$ is the linear term, which is to suppress dynamic vanishing noise, $\tau_2\text{sign}(e)$ is the discontinuous term, which is to suppress dynamic non-vanishing noise, the design idea of adding the discontinuous term is inspired by literature [41]. In this literature, to deal with noises in slid mode control, discontinuous terms are universally used. Then, substituting the error function into (2), the MNAZND model for solving the CDMI can be obtained as

$$\Phi(t)\dot{Z}(t) = -\dot{\Phi}(t)Z(t) - \sigma\mathfrak{A}(\Phi(t)Z(t) - I). \tag{5}$$

In addition, the perturbed MNAZND model by additional noise is described as

$$\Phi(t)\dot{Z}(t) = -\dot{\Phi}(t)Z(t) - \sigma\mathfrak{A}(\Phi(t)Z(t) - I) + \Psi(t), \tag{6}$$

where $\Psi(t)$ denotes additional noise. The MNAZND model with the proposed NV-AF(4) can not only have a explicitly given convergence time but also can endure various noises (including bounded vanishing noise, bounded non-vanishing noise) in fixed time.

III. THEORETICAL ANALYSIS

In this section, we mainly present the theoretical results of the MNAZND model. At first, the global stability and fixed time convergence of the MNAZND model are proven in theory. Then, the robustness of the MNAZND model is discussed by analyzing the perturbed MNAZND model with unknown additive noises.

A. GLOBAL STABILITY

Theorem 1: Given a complex-valued time-varying matrix $\Phi(t)$ of full rank, the state matrix $Z(t)$ synthesized by the MNAZND model (5) with NV-AF (4), starting from any stochastic initial state $Z(0)$, always converges to theoretical solution of Eqn.(1), i.e. the error matrix $\mathfrak{D}(t)$ global converges to 0.

Proof: Based on Eqn.(2), element-wise, we have

$$\dot{\mathfrak{D}}_{mn}(t) = -\sigma\mathfrak{A}(\mathfrak{D}_{mn}(t)),$$

then, we construct a Lyapunov function

$$\omega_{mn}(t) = |\mathfrak{D}_{mn}(t)|^2 = \mathfrak{D}_{mn}(t)\overline{\mathfrak{D}_{mn}(t)},$$

where $|\mathfrak{D}_{mn}(t)|$ denotes the modulus of $\mathfrak{D}_{mn}(t)$. The derivative of $\omega_{mn}(t)$ can be written as

$$\begin{aligned}\dot{\omega}_{mn}(t) &= \dot{\mathfrak{D}}_{mn}(t)\overline{\mathfrak{D}_{ij}(t)} + \mathfrak{D}_{mn}(t)\overline{\dot{\mathfrak{D}}_{mn}(t)}. \\ &= -\sigma\mathfrak{A}(\mathfrak{D}_{mn}(t))\overline{\mathfrak{D}_{mn}(t)} - \sigma\mathfrak{D}_{mn}(t)\mathfrak{A}(\overline{\mathfrak{D}_{mn}(t)}).\end{aligned} \tag{7}$$

According to the definition of the complex-valued activation type $\mathfrak{A}(\cdot)$ in (3), we have

$$\begin{aligned}\dot{\omega}_{mn}(t) &= -\sigma\overline{\mathfrak{D}_{mn}(t)}\mathbb{J}(|\mathfrak{D}_{mn}(t)|)\exp(i\theta)\\ &\quad -\sigma\mathfrak{D}_{mn}(t)\mathbb{J}(|\mathfrak{D}_{mn}(t)|)\exp(-i\theta)\\ &= -\sigma|\mathfrak{D}_{mn}(t)|\exp(-i\theta)\mathbb{J}(|\mathfrak{D}_{mn}(t)|)\exp(i\theta)\\ &\quad -\sigma|\mathfrak{D}_{mn}(t)|\exp(i\theta)\mathbb{J}(|\mathfrak{D}_{mn}(t)|)\exp(-i\theta)\\ &= -2\sigma|\mathfrak{D}_{mn}(t)|\mathbb{J}(|\mathfrak{D}_{mn}(t)|), \end{aligned} \tag{8}$$

where θ denotes the argument of $\mathfrak{D}_{mn}(t)$, apparently, $\dot{\omega}_{mn}(t)$ is negative definite, so $\mathfrak{D}_{mn}(t)$ globally converges to 0. Therefore, the error matrix $\mathfrak{D}(t)$ global converges to 0 is proven. □

B. FIXED TIME CONVERGENCE

Theorem 2: Given a complex-valued time-varying matrix $\Phi(t)$ of full rank, the state matrix $Z(t)$ synthesized by the MNAZND model (5) with NV-AF (4), starting from any stochastic initial state $Z(0)$, can converge to theoretical solution of Eqn.(1) in fixed time t_f.

$$t_f \leq \frac{1}{\sigma\tau_1}.$$

Proof: Same as **Theorem 1**, we also have $\dot{\mathfrak{D}}_{mn}(t) = -\sigma\mathfrak{A}(\mathfrak{D}_{mn}(t))$, and also construct the Lyapunov function as $\omega_{mn}(t) = |\mathfrak{D}_{mn}(t)|^2 = \mathfrak{D}_{mn}(t)\overline{\mathfrak{D}_{mn}(t)}$. According to Eqs. (7) and (8), we have

$$\begin{aligned}\dot{\omega}_{mn}(t) &= -2\sigma|\mathfrak{D}_{mn}(t)|\mathbb{J}(|\mathfrak{D}_{mn}(t)|)\\ &= -2\sigma|\mathfrak{D}_{mn}(t)|(\tau_1\exp(|\mathfrak{D}_{mn}(t)|^k)|\mathfrak{D}_{mn}(t)|^{1-k}/k\\ &\quad +\tau_2+\tau_3|\mathfrak{D}_{mn}(t)|)\\ &\leq -2\sigma|\mathfrak{D}_{mn}(t)|\tau_1\exp(|\mathfrak{D}_{mn}(t)|^k)|\mathfrak{D}_{mn}(t)|^{1-k}/k\\ &= -\sigma\tau_1\exp(\omega_{mn}(t)^{\frac{k}{2}})\omega_{mn}(t)^{1-\frac{k}{2}}/\frac{k}{2}.\end{aligned}$$

That is

$$\frac{1}{\sigma\tau_1}\frac{k}{2}\exp(-\omega_{mn}(t)^{\frac{k}{2}})\omega_{mn}(t)^{\frac{k}{2}-1}\mathrm{d}\omega_{mn}(t) \geq \mathrm{d}t. \tag{9}$$

Integrating on both sides of (9), we obtain

$$t_f \leq \frac{1-\exp(-\omega_{mn}(0)^{\frac{k}{2}})}{\sigma\tau_1} = \frac{1-\exp(-|\mathfrak{D}_{mn}(0)|^k)}{\sigma\tau_1}. \tag{10}$$

Since $0 < \exp(-|\mathfrak{D}_{mn}(0)|^k) \leq 1$, the fixed convergence time is

$$t_f \leq \frac{1}{\sigma\tau_1}.$$

Therefore, the MNAZNN model (5) activated by NV-AF (4) can exhibit a fixed time convergence. □

C. ROBUSTNESS ANALYSIS

When the perturbed MNAZND model (6) is inlaid the NV-AF (4) with dynamic bounded noise or large constant noise, the robustness analysis can be inferred by following theorems.

Theorem 3: Given a complex-valued time-varying matrix $\Phi(t)$ of full rank and dynamic bounded time-varying noise $\Psi(t)$ with its element satisfying $|\psi_{mn}(t)| \leq \rho$ ($\rho \geq 0$), and the NV-AF (4) with $\sigma\tau_2 \geq \rho$, the state matrix $Z(t)$ synthesized by the perturbed MNAZND model (6) with the NV-AF (4), starting from stochastic initial $Z(0)$, can converge to theoretical solution in fixed time t_f.

$$t_f \leq \frac{1}{\sigma\tau_1}.$$

Proof: According to the error matrix $\mathfrak{D}(t)$, when choosing the activated type $\mathfrak{A}(t)(\cdot)$ in (3), element-wise, we get

$$\dot{\mathfrak{D}}_{mn}(t) = -\sigma\mathfrak{A}(\mathfrak{D}_{mn}(t)) + \psi_{mn}(t).$$

To prove the robustness, we also construct a Lyapunov function $\omega_{mn}(t) = |\mathfrak{D}_{mn}(t)|^2 = \mathfrak{D}_{mn}(t)\overline{\mathfrak{D}_{mn}(t)}$, $\theta = \arg(\mathfrak{D}_{mn}(t))$. Then, we have

$$\begin{aligned}\dot{\omega}_{mn}(t) &= \overline{\mathfrak{D}_{mn}(t)}\big(-\sigma\mathfrak{A}(\mathfrak{D}_{mn}(t)) + \psi_{mn}(t)\big)\\ &\quad +\mathfrak{D}_{mn}(t)\big(-\sigma\mathfrak{A}(\overline{\mathfrak{D}_{mn}(t)}) + \overline{\psi_{mn}(t)}\big)\\ &= -\sigma\overline{\mathfrak{D}_{mn}(t)}\mathbb{J}(|\mathfrak{D}_{mn}(t)|)\exp(i\theta) + \overline{\mathfrak{D}_{mn}(t)}\psi_{mn}(t)\\ &\quad -\sigma\mathfrak{D}_{mn}(t)\mathbb{J}(|\mathfrak{D}_{mn}(t)|)\exp(-i\theta) + \mathfrak{D}_{mn}(t)\overline{\psi_{mn}(t)}\\ &= -2\sigma|\mathfrak{D}_{mn}(t)|\mathbb{J}(|\mathfrak{D}_{mn}(t)|)\\ &\quad +\overline{\mathfrak{D}_{mn}(t)}\psi_{mn}(t) + \mathfrak{D}_{mn}(t)\overline{\psi_{mn}(t)}\\ &= -2\sigma|\mathfrak{D}_{mn}(t)|\exp(|\mathfrak{D}_{mn}(t)|^k)|\mathfrak{D}_{mn}(t)|^{1-k}/k\\ &\quad -2\sigma\tau_3|\mathfrak{D}_{mn}(t)|^2 + \overline{\mathfrak{D}_{mn}(t)}\psi_{mn}(t)\\ &\quad +\mathfrak{D}_{mn}(t)\overline{\psi_{mn}(t)} - 2\sigma\tau_2|\mathfrak{D}_{mn}(t)|\\ &\leq -2\sigma|\mathfrak{D}_{mn}(t)|\exp(|\mathfrak{D}_{mn}(t)|^k)|\mathfrak{D}_{mn}(t)|^{1-k}/k\\ &\quad +2|\mathfrak{D}_{mn}(t)|(|\psi_{mn}(t)| - \sigma\tau_2)\\ &\leq -2\sigma|\mathfrak{D}_{mn}(t)|\exp(|\mathfrak{D}_{mn}(t)|^k)|\mathfrak{D}_{mn}(t)|^{1-k}/k\\ &\quad +2|\mathfrak{D}_{mn}(t)|(\rho - \sigma\tau_2)\\ &\leq -2\sigma|\mathfrak{D}_{mn}(t)|\exp(|\mathfrak{D}_{mn}(t)|^k)|\mathfrak{D}_{mn}(t)|^{1-k}/k\\ &= -\sigma\tau_1\exp(\omega_{mn}(t)^{\frac{k}{2}})\omega_{mn}(t)^{1-\frac{k}{2}}/\frac{k}{2}.\end{aligned}$$

Hence, when the perturbed MNAZND model (6) with dynamic bounded noise, according to Eqn.(9) and Eqn.(10) in **Theorem 2**, the fixed convergence time can be gotten as

$$t_f \leq \frac{1}{\sigma\tau_1}.$$

Therefore, the perturbed MNAZND model (6) activated by NV-AF (4) under a dynamic bounded noise still exhibits a fixed time convergence. □

Theorem 4: Given a complex-valued time-varying matrix $\Phi(t)$ of full rank and a large fixed constant noise $\Psi(t) = L$, that is, $\exists\varepsilon, \sigma \ll \varepsilon \ll +\infty, L \leq \varepsilon$, as the time goes, the Frobenius norm of the error function $\|\mathfrak{D}_{mn}(t)\|_F$ synthesized by the perturbed MNAZND model (6) with the NV-AF (4) satisfies the inequality as:

$$\lim_{t\to+\infty}\|\mathfrak{D}_{mn}(t)\|_F \leq q\left(\frac{k^{2L}\Pi_{\iota=0}^{L-1}(\iota!)^2}{(L+2)^{L+2}\tau_1^{2L}(\tau_2\tau_3)^2}\right)^{\frac{1}{\varpi}}\left(\frac{\varepsilon}{\sigma}\right)^{\frac{2L+4}{\varpi}},$$

where $\varpi = Lk(L-3) + 2(L+1)$.

Proof: Firstly, a Lyapunov function $\omega_{mn}(t) = |\mathfrak{D}_{mn}(t)|^2/2$ is constructed. According to $\dot{\mathfrak{D}}_{mn}(t) = -\sigma\mathfrak{A}(\mathfrak{D}_{mn}(t)) + \Psi(t)$ and the large fixed constant noise L, the time derivation of $\omega_{mn}(t)$ is

$$\begin{aligned}\dot{\omega}_{mn}(t) &= \frac{1}{2}\big(\overline{\mathfrak{D}_{mn}(t)}\big(-\sigma\mathfrak{A}(\mathfrak{D}_{mn}(t)) + L\big) \\ &\quad + \mathfrak{D}_{mn}(t)\big(-\sigma\mathfrak{A}(\overline{\mathfrak{D}_{mn}(t)}) + \overline{L}\big)\big) \\ &= -\frac{1}{2}\big(\sigma\overline{\mathfrak{D}_{mn}(t)}\mathbb{J}(|\mathfrak{D}_{mn}(t)|)\exp(i\theta) + \overline{\mathfrak{D}_{mn}(t)}L \\ &\quad - \sigma\mathfrak{D}_{mn}(t)\mathbb{J}(|\mathfrak{D}_{mn}(t)|)\exp(-i\theta) + \mathfrak{D}_{mn}(t)\overline{L}\big) \\ &\le -\sigma|\mathfrak{D}_{mn}(t)|\mathbb{J}(|\mathfrak{D}_{mn}(t)|) + |\mathfrak{D}_{mn}(t)||L| \\ &\le -|\mathfrak{D}_{mn}(t)|(\sigma\mathbb{J}(|\mathfrak{D}_{mn}(t)|) - \varepsilon).\end{aligned}$$

According to [42], we have $\lim_{t\to+\infty}\mathbb{J}(|\mathfrak{D}_{mn}(t)|) \approx \varepsilon/\sigma$. Then, we can get

$$\begin{aligned}&\lim_{t\to+\infty}\mathbb{J}^2(|\mathfrak{D}_{mn}(t)|) \\ &= \lim_{t\to+\infty}\Bigg(\tau_1\exp(|\mathfrak{D}_{mn}(t)|^k)|\mathfrak{D}_{mn}(t)|^{1-k}/k \\ &\quad + \tau_2 + \tau_3|\mathfrak{D}_{mn}(t)|\Bigg)^2 \\ &= \lim_{t\to+\infty}\left(\frac{\tau_1}{k}\sum_{\iota=0}^{+\infty}\frac{|\mathfrak{D}_{mn}(t)|^{1+(\iota-1)k}}{\iota!} + \tau_3|\mathfrak{D}_{mn}(t)| + \tau_2\right)^2 \\ &\ge \lim_{t\to+\infty}\left(\frac{\tau_1}{k}\sum_{\iota=0}^{L-1}\frac{|\mathfrak{D}_{mn}(t)|^{1+(\iota-1)k}}{\iota!} + \tau_3|\mathfrak{D}_{mn}(t)| + \tau_2\right)^2 \\ &\ge \lim_{t\to+\infty}\Bigg((\frac{\tau_1}{k})^2\sum_{\iota=0}^{L-1}\frac{|\mathfrak{D}_{mn}(t)|^{2+2(\iota-1)k}}{\iota!^2} \\ &\quad + (\tau_3|\mathfrak{D}_{mn}(t)|)^2 + \tau_2^2\Bigg)^2 \\ &\ge \lim_{t\to+\infty}(L+2)(\frac{\tau_1}{k})^{2L}\big((\tau_2\tau_3)^2\Pi_{\iota=0}^{L-1}\frac{|\mathfrak{D}_{mn}(t)|^{\varpi}}{(\iota!)^2}\big)^{\frac{1}{L+2}},\end{aligned}$$

where $\varpi = Lk(L-3) + 2(L+1)$, then

$$\lim_{t\to+\infty}|\mathfrak{D}_{mn}(t)|^2 \le \left(\frac{k^{2L}\Pi_{\iota=0}^{L-1}(\iota!)^2}{(L+2)^{L+2}\tau_1^{2L}(\tau_2\tau_3)^2}\right)^{\frac{2}{\varpi}}\left(\frac{\varepsilon}{\sigma}\right)^{\frac{4L+8}{\varpi}}.$$

Hence, we finally get

$$\lim_{t\to+\infty}\|\mathfrak{D}_{mn}(t)\|_F \le q\left(\frac{k^{2L}\Pi_{\iota=0}^{L-1}(\iota!)^2}{(L+2)^{L+2}\tau_1^{2L}(\tau_2\tau_3)^2}\right)^{\frac{1}{\varpi}}\left(\frac{\varepsilon}{\sigma}\right)^{\frac{2L+4}{\varpi}}.$$

The proof completes. □

IV. NUMERICAL EXPERIMENTS AND APPLICATION

For computing CDMI efficiently, the MNAZND model embedded the NV-AF is mentioned in Section II. In addition, we comprehensively analyze the performance of the MNAZND model, including global stability, fixed time convergence and noise resistance in Section III. In this section, numerical examples will be adopted to authenticate the comprehensive performance of the MNAZND model.

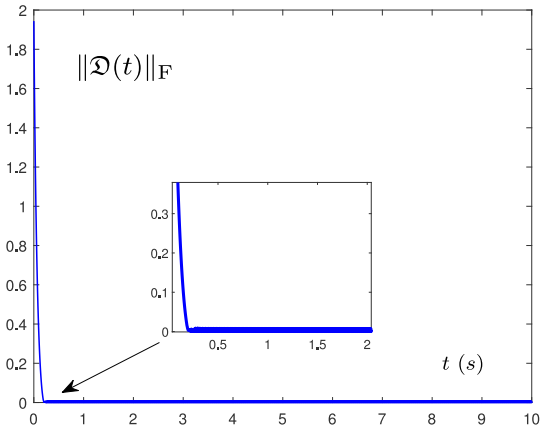

FIGURE 1. The residual error of $Z(t)$ synthesized by the proposed MNAZND model with the NV-AF.

A. EXAMPLE 1

Let's first adopt a relatively simple complex-valued time-varying matrix $\Phi(t)$ as following:

$$\Phi(t) = \begin{bmatrix} e^{it} & -ie^{-it} \\ -ie^{it} & e^{-it} \end{bmatrix} \in \mathbb{C}^{2\times 2}, \tag{11}$$

the theoretical solution of $\Phi(t)$ can be easily gotten by mathematical calculations,

$$\Phi^{-1}(t) = \frac{1}{2}\begin{bmatrix} e^{-it} & ie^{-it} \\ ie^{it} & e^{it} \end{bmatrix}.$$

We first check the effectiveness and accuracy of the MNAZND model (5) activated by NV-AF (4). In this example, the parameters in the MNAZND model are set as $\tau_1 = \tau_2 = \tau_3 = 1$, $k = 1/2$, and $\sigma = 2$. According to **Theorem 2**, we can get the fixed convergence time as: $t_{\mathrm{f}} \le 1/(\sigma\tau_1) = 0.5s$. From Fig. 1, the convergence time approximately is $0.2s$, which is less than theoretical fixed time $t_{\mathrm{f}} = 0.5s$. Fig. 2 shows the trajectories synthesized by MNAZND model, In Fig. 2(a), starting from a randomly initial state $Z(0)$, the blue trajectories $Z(t)$ synthesized by the MNAZND model coincide with the theoretical solution precisely and rapidly. Fig. 2(b) depicts the profile of trajectories. The simulation results verify theoretical derivation in **Theorem 1** and **2**.

According to [35], [38], and [37], L-AF $\mathbb{J}_1(e) = e$ and NL-AFs (mainly including SBP-AF $\mathbb{J}_2(e) = (|e|^k + |e|^{\frac{1}{k}})\mathrm{sign}(e)$ and OSBP-AF $\mathbb{J}_3(e) = \alpha\mathrm{sign}^k(e) + \beta e$) were used for improving converge speed. In this section, to demonstrate the advantage of NV-AF (4), aforementioned existing NL-AFs are implanted in MNAZND model. Fig. 3 shows the residual errors synthesized by the MNAZND model under different situations. To make this a fair comparison, the same initial value of $Z(t)$ is set under same situation. Fig. 3(a) depicts that shorter converge time can be obtained by employing NV-AF (4) in free noise situation, the actual time of the residual error decreases to zero is less than the theoretical fixed time $0.5s$. Fig. 3(b) and Fig. 3(c) respectively shows convergence situations under dynamic vanishing noise and dynamic bounded noise. In these cases,

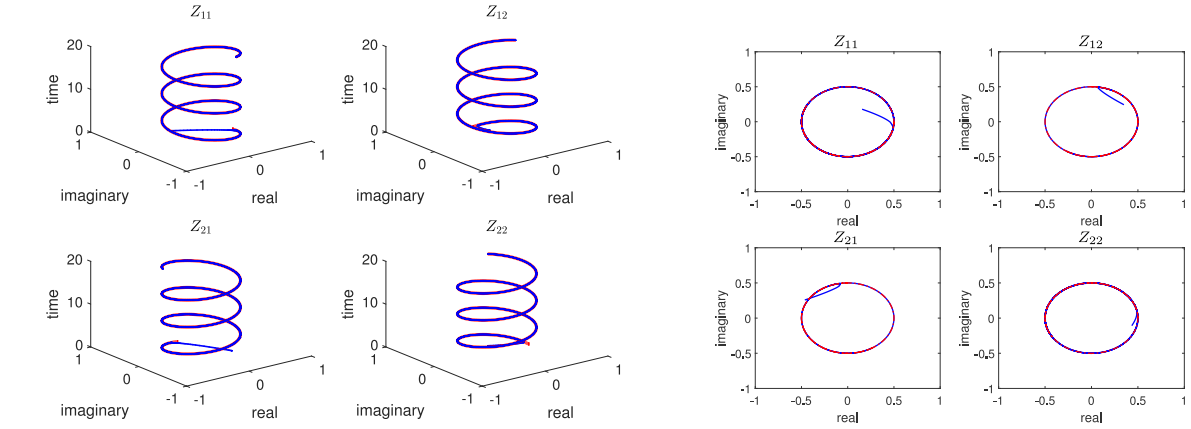

(a) (b)

FIGURE 2. Dynamic trajectories of $Z(t)$ synthesized by the proposed MNAZND model with the NV-AF. (a) Dynamic trajectories. (b) Profile of dynamic trajectories.

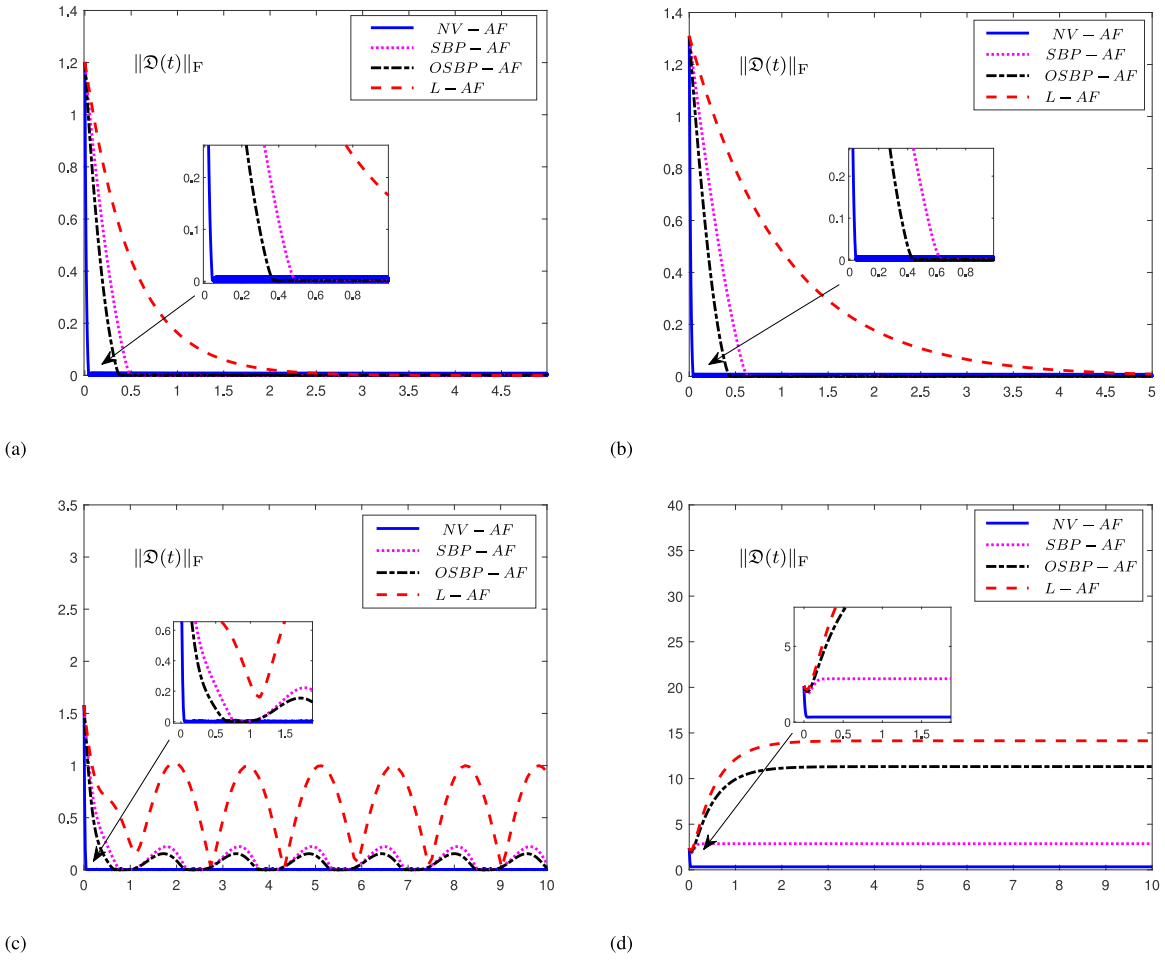

(a) (b) (c) (d)

FIGURE 3. The residual error of $Z(t)$ (11) synthesized by the MNAZND model with different AFs. (a) Free noise. (b) $\Psi(t) = \mathfrak{D}_{mn}(t)$. (c) $\Psi(t) = cos(2t) + cos(2t)i$. (d) $\Psi(t) = 10 + 10i$.

the converge speed of the MNAZND model embedded NV-AF (4) almost same as the free situation. The numerical experiment results validate the analysis of **Theorem 2** and **3**. In contrast, the MNAZND model embedded L-AF, SBP-AF and OSBP-AF cannot vanish to zero under dynamic bounded noise. In Fig. 3(d), compared with the aforementioned existing popular NL-AFs under the constant noise situation, the NV-AF (4) also obtains the best performance.

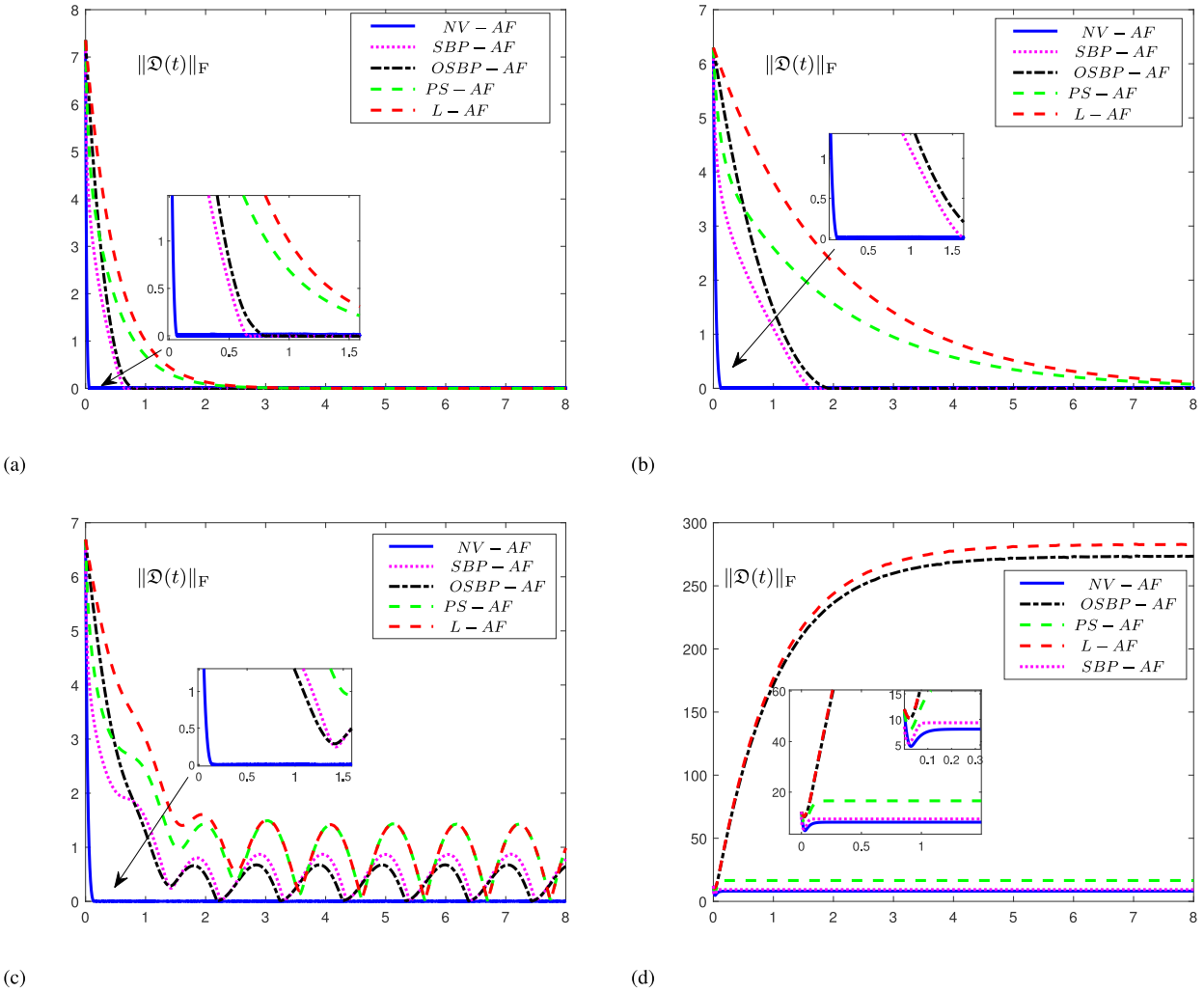

FIGURE 4. The residual error of $Z(t)$ (11) synthesized by the MNAZND model with different AFs. (a) Free noise. (b) $\Psi(t) = 0.5\mathfrak{D}_{mn}(t)$. (c) $\Psi(t) = 0.8sin(3t) + 0.8sin(3t)i$. (d) $\Psi(t) = 50 + 50i$.

B. EXAMPLE 2

To further investigate the superiority of the MNAZND model (5) activated by NV-AF (4), a more complicated complex-valued time-varying matrix is considered as following.

$$\Phi(t) = \begin{bmatrix} \phi_{11}(t) & \phi_{12}(t) & \cdots & \phi_{1q}(t) \\ \phi_{21}(t) & \phi_{22}(t) & \cdots & \phi_{2q}(t) \\ \vdots & \vdots & \ddots & \vdots \\ \phi_{q1}(t) & \phi_{q2}(t) & \cdots & \phi_{qq}(t) \end{bmatrix} \tag{12}$$

with $\phi_{mn}(t)$ denotes the mnth element of $\phi(t)$, and

$$\phi_{mn}(t) = \begin{cases} 2sin(3t)i, & m = n, \\ n - 1 + 2cos(3t)i, & m < n, \\ n + 2cos(3t)i, & m > n. \end{cases}$$

In the simulation, the dimension of the matrix $\Phi(t)$ equals 4, the relevant parameters are set as $\sigma = 1, \tau_1 = \tau_2 = \tau_3 = 2$ and $k = 1/2$. According to theoretical analysis result, the theoretical fixed convergence time $t_{\mathrm{up}} \leq 1/(\sigma\tau_1) = 0.5s$ can be obtained in free noise, dynamic vanishing noise and bounded noise. According to the PS-AF also have good performance in some situation [36], so in this example, PS-AF is employed for comparison. The corresponding experimental results are demonstrated in Fig. 4, which substantiates that NV-AF (4) endows ZND model a superior stability, convergence and robustness under different situations than other NL-AFs. Thereinto, from Fig. 4(a) to Fig. 4(c), the convergence time of the perturbed MNAZND model (6) activated by NV-AF (4) is almost the same, about $0.2s$, which satisfies the theoretical fixed convergence time $0.5s$. In Fig. 4(d), under a large constant noise, the residual error of the perturbed MNAZND model (5) activated by NV-AF (4) remains in a smallest stable level, which further validates advantage of NV-AF (4).

As pointed in [35], the parameter σ can scale the convergence of the ZND model. Therefore, in this part, we further investigate the convergence performance of the

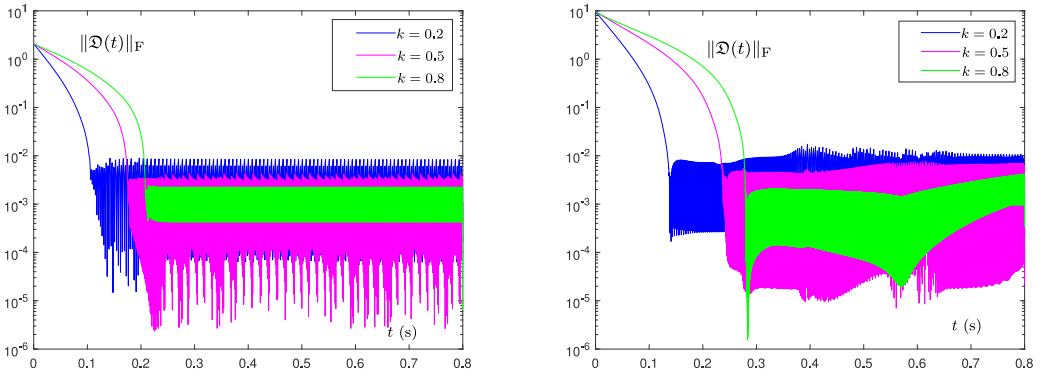

FIGURE 5. The residual error of the examples synthesized by the MNAZND model with different values of parameter k. (a) Example 1. (b) Example 2.

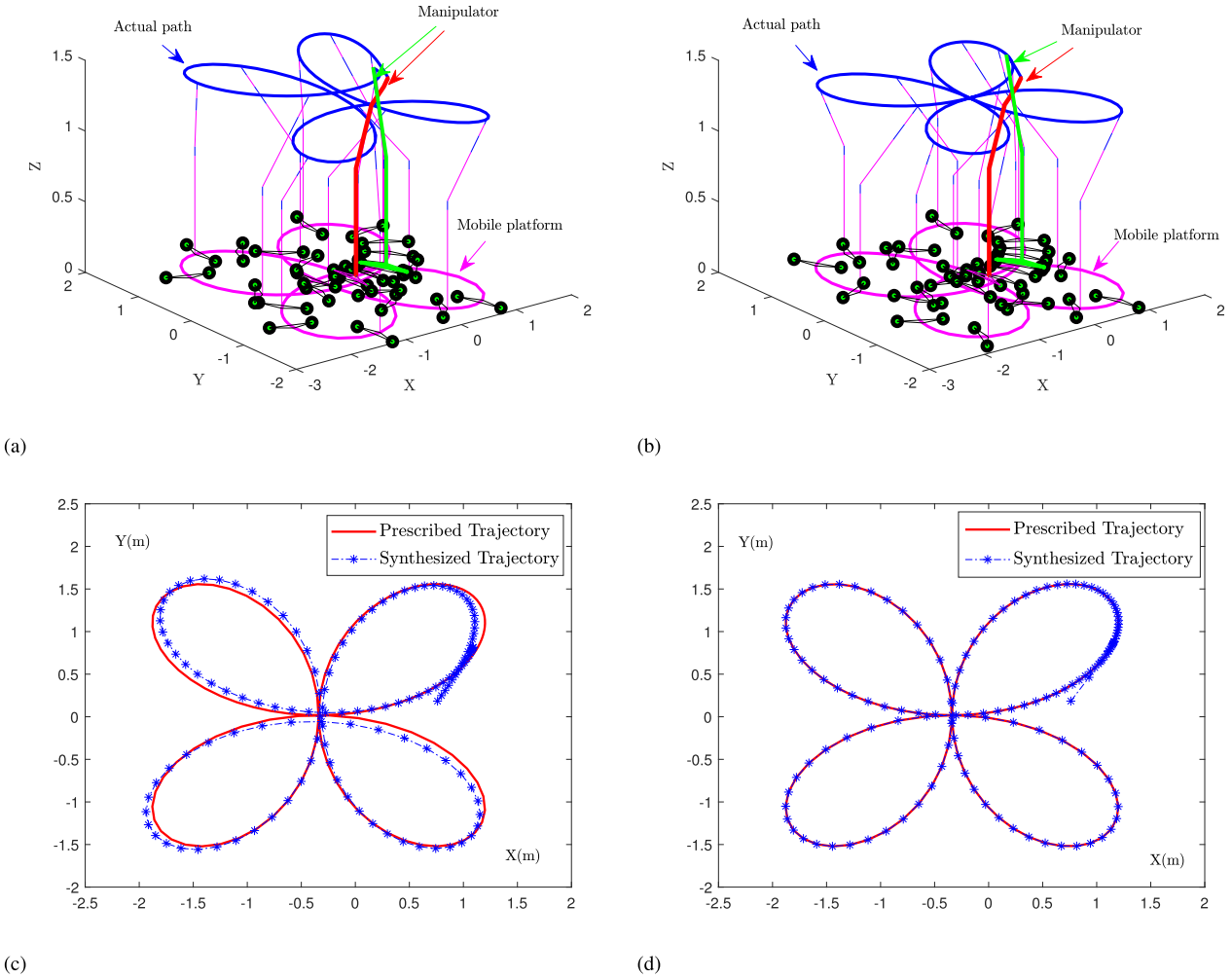

FIGURE 6. The space and the end effector trajectories. (a-b) controlled by CZND. (c-d) controlled by MNAZND.

MNAZND model (5) at different parameters value. Based on the structure of the NV-AF (4), $\tau_1 \exp(|e|^k)|e|^{1-k}\mathrm{sign}(e)/k$ is the original term, which is to ensure fixed time convergence. Obviously, as to the convergence speed, the parameter τ_1 is the same as σ, larger value of τ_1 achieves faster convergence speed. For the tunable parameter k, set different values,

the convergence effect of Example 1 and 2 is respectively shown in Fig. 5(a) and Fig. 5(b), from the simulation results, it is suggested that a small value of k accelerates the convergence.

C. APPLICATION

In order to verify the effectiveness of the proposed MNAZND in actual application, a robotic manipulator controlling is employed in this section. According to [14], the position of the end effector is a vital control component, and the kinematical model of which can be represented as follows:

$$\Upsilon(t) = \mathbb{J}(\Xi(t)) \in \mathbb{R}^k,$$

where $\Xi(t) = [\hbar^T(t), \Theta^T(t)]^T \in \mathbb{R}^{l+2}$ includes the two angle vectors, thereinto, $\hbar^T(t)$ denotes the mobile platform angle vector, $\Theta^T(t)$ denotes the manipulator angle vector, $\Upsilon(t)$ is the actual position of end effector in three dimensions. and $\mathbb{J}(\cdot)$ is a nonlinear mapping from $\Xi(t)$ to $\Upsilon(t)$.

Based on the dynamics control principle of the designed MNAZND, a kinetic equation can be obtained as:

$$\mathbb{W}(\Xi(t))\dot{\Xi}(t) = \dot{\Upsilon}(t) - \sigma\mathbb{J}(\Upsilon(t) - \Xi(t)),$$

where $\mathbb{W}(\Xi(t)) = \partial\Upsilon(\Xi(t))/\partial\Xi \in \mathbb{R}^{k\times(l+2)}$. The feasibility of the designed method will be verified by controlling the end effector of a mobile manipulator to track a prescribed route. In this simulation, four leaf clover trajectory is be tracked, In order to contrast the reliability, the classic ZND (CZND) is introduced, and the parameters in the dynamics control system are set as: $\sigma = 2$, $\tau_1 = \tau_2 = \tau_3 = k = 1/2$, $\Xi(0) = [0, 0, \pi/12, \pi/4, \pi/6, \pi/6, \pi/8, \pi/3]$, the corresponding results are demonstrated in Figure 6. Figure 6 shows the mobile manipulators' tracking consequence controlled by the CZND model and MNAZND model in a noise environment ($\Psi(t) = 0.2sin2t$). The entire space trajectories of the mobile manipulator controlled by the CZND model and MNAZND model are respectively depicted in Fig. 6(a) and Fig. 6(b), and the end effector trajectories synthesized by the CZND model and MNAZND model are respectively depicted in Fig. 6(c) and Fig. 6(d). Obviously, the mobile manipulator controlled by MNAZND can satisfactorily complete the four leaf clover trajectory tracking task in noise disturbed state.

V. CONCLUSION

A MNAZND model with NV-AF is proposed to solve the noise disturbed CDMI. Unlike the existing ZND model, the NL-AF consists of three terms. The function of each term endows the MNAZND model can simultaneously achieve fixed time convergence and robustness. The stability, fixed-time convergence and robustness of the MNAZND model with NV-AF are proven theoretically. Furthermore, the fixed time convergence upper bound is obtained, which is independent of the initial value and keeps same in free noise and bounded dynamic noise. The illustrative examples and the application on robotic manipulator verified that the MNAZND model with NV-AF has a more remarkable performance. Compared with the real-valued and complex-valued ZND models, the quaternion-valued ZND model has competitive advantage in storage capacity. Therefore, the research of applying the MNAZND model in quaternion field is a worthy direction.

Conflicts of Interest: The authors declare no conflict of interest.

REFERENCES

[1] T. Kohonen, G. Barna, and R. Chrisley, "Statistical pattern recognition with neural networks: Benchmarking studies," in *Proc. IEEE Int. Conf. Neural Netw.*, Jun. 1988, pp. 61–68.
[2] H. Lin, Y. Tian, J. Hou, W. Xu, X. Shi, and R. Tang, "Fussy inverse design of metamaterial absorbers assisted by a generative adversarial network," *Frontiers Mater.*, vol. 9, p. 9, Jul. 2022, doi: 10.3389/fmats.2022.926094. [Online]. Available: https://www.frontiersin.org/articles/10.3389/fmats.2022.926094/full
[3] B. Gu and V. S. Sheng, "Statistical pattern recognition with neural networks: Benchmarking studies," *IEEE Trans. Neural Netw. Learn. Syst.*, vol. 24, no. 8, pp. 1304–1315, Aug. 2013.
[4] D. Guo and Y. Zhang, "Zhang neural network, Getz–Marsden dynamic system, and discrete-time algorithms for time-varying matrix inversion with application to robots' kinematic control," *Neurocomputing*, vol. 97, pp. 22–32, Nov. 2012.
[5] L. Jin, Y. Zhang, and S. Li, "Integration-enhanced Zhang neural network for real-time-varying matrix inversion in the presence of various kinds of noises," *IEEE Trans. Neural Netw. Learn. Syst.*, vol. 27, no. 12, pp. 2615–2627, Dec. 2016.
[6] F. J. Pinski, G. Simpson, A. M. Stuart, and H. Weber, "Kullback–Leibler approximation for probability measures on infinite dimensional spaces," *SIAM J. Math. Anal.*, vol. 47, no. 6, pp. 4091–4122, Jan. 2015.
[7] Y. Liu, C. Duan, L. Liu, and L. Cao, "Discrete-time incremental backstepping control with extended Kalman filter for UAVs," *Electronics*, vol. 12, no. 14, p. 3079, Jul. 2023.
[8] H. Li and R. O. Foschi, "An inverse reliability method and its application," *Structural Saf.*, vol. 20, no. 3, pp. 257–270, Sep. 1998.
[9] L. Ma, K. Dickson, J. McAllister, and J. McCanny, "QR decomposition-based matrix inversion for high performance embedded MIMO receivers," *IEEE Trans. Signal Process.*, vol. 59, no. 4, pp. 1858–1867, Apr. 2011.
[10] P. S. Stanimirović, M. Ć irić, I. Stojanović, and D. Gerontitis, "Conditions for existence, representations, and computation of matrix generalized inverses," *Complexity*, vol. 2017, no. 1, 2017, Art. no. 6429725.
[11] Z. Yu, Y. Sun, J. Zhang, Y. Zhang, and Z. Liu, "Gated recurrent unit neural network (GRU) based on quantile regression (QR) predicts reservoir parameters through well logging data," *Frontiers Earth Sci.*, vol. 11, p. 8, Jan. 2023, doi: 10.3389/feart.2023.1087385. [Online]. Available: https://www.frontiersin.org/articles/10.3389/feart.2023.1087385/full
[12] W. E. Leithead and Y. Zhang, "$O(N^2)$-operation approximation of covariance matrix inverse in Gaussian process regression based on quasi-Newton BFGS method," *Commun. Statist. Simul. Comput.*, vol. 36, no. 2, pp. 367–380, 2007.
[13] H. Ramos and M. Monteiro, "A new approach based on the Newton's method to solve systems of nonlinear equations," *J. Comput. Appl. Math.*, vol. 318, pp. 3–13, Jul. 2017.
[14] B. Liao, Y. Wang, J. Li, D. Guo, and Y. He, "Harmonic noise-tolerant ZNN for dynamic matrix pseudoinversion and its application to robot manipulator," *Frontiers Neurorobotics*, vol. 16, Jun. 2022, Art. no. 928636.
[15] X.-Z. Wang, H. Ma, and P. S. Stanimirović, "Recurrent neural network for computing the W-weighted Drazin inverse," *Appl. Math. Comput.*, vol. 300, pp. 1–20, May 2017.
[16] W. Chen, J. Jin, D. Gerontitis, L. Qiu, and J. Zhu, "Improved recurrent neural networks for text classification and dynamic Sylvester equation solving," *Neural Process. Lett.*, vol. 55, no. 7, pp. 8755–8784, Dec. 2023.
[17] L. Su and L. Zhou, "Exponential synchronization of memristor-based recurrent neural networks with multi-proportional delays," *Neural Comput. Appl.*, vol. 31, no. 11, pp. 7907–7920, Nov. 2019.
[18] J. Lu, W. Li, J. Sun, R. Xiao, and B. Liao, "Secure and real-time traceable data sharing in cloud-assisted IoT," *IEEE Internet Things J.*, vol. 11, no. 4, pp. 6521–6536, Feb. 2024.

[19] W. Li, L. Han, X. Xiao, B. Liao, and C. Peng, "A gradient-based neural network accelerated for vision-based control of an RCM-constrained surgical endoscope robot," *Neural Comput. Appl.*, vol. 34, no. 2, pp. 1329–1343, Jan. 2022.
[20] Y. Zhang, S. Li, J. Weng, and B. Liao, "GNN model for time-varying matrix inversion with robust finite-time convergence," *IEEE Trans. Neural Netw. Learn. Syst.*, vol. 35, no. 1, pp. 559–569, Jan. 2024.
[21] D. Guo, C. Yi, and Y. Zhang, "Zhang neural network versus gradient-based neural network for time-varying linear matrix equation solving," *Neurocomputing*, vol. 74, no. 17, pp. 3708–3712, Oct. 2011.
[22] Y. Zhang and S. S. Ge, "Design and analysis of a general recurrent neural network model for time-varying matrix inversion," *IEEE Trans. Neural Netw.*, vol. 16, no. 6, pp. 1477–1490, Nov. 2005.
[23] S. Li, S. Chen, and B. Liu, "Accelerating a recurrent neural network to finite-time convergence for solving time-varying Sylvester equation by using a sign-bi-power activation function," *Neural Process. Lett.*, vol. 37, no. 2, pp. 189–205, Apr. 2013.
[24] B. Liao, L. Han, X. Cao, S. Li, and J. Li, "Double integral-enhanced zeroing neural network with linear noise rejection for time-varying matrix inverse," *CAAI Trans. Intell. Technol.*, vol. 1, no. 1, pp. 1–14, 2022.
[25] J. Dai, P. Tan, L. Xiao, L. Jia, Y. He, and J. Luo, "A fuzzy adaptive zeroing neural network model with event-triggered control for time-varying matrix inversion," *IEEE Trans. Fuzzy Syst.*, vol. 31, no. 11, pp. 3974–3983, Nov. 2023.
[26] L. Xiao, J. Luo, Y. Ning, J. Li, and P. Tan, "Fixed-time, robust and fuzzy adaptive consensus control with event trigger mechanism based on a novel ZNN scheme," *Res. Square*, vol. 11, no. 99, pp. 1–10, 2023.
[27] Y. Liufu, L. Jin, M. Shang, X. Wang, and F.-Y. Wang, "ACP-incorporated perturbation-resistant neural dynamics controller for autonomous vehicles," *IEEE Trans. Intell. Vehicles*, vol. 9, no. 4, pp. 4675–4686, Apr. 2024.
[28] L. Jin, L. Liu, X. Wang, M. Shang, and F.-Y. Wang, "Physical-informed neural network for MPC-based trajectory tracking of vehicles with noise considered," *IEEE Trans. Intell. Vehicles*, vol. 9, no. 3, pp. 4493–4503, Mar. 2024.
[29] B. Liao, C. Hua, Q. Xu, X. Cao, and S. Li, "Inter-robot management via neighboring robot sensing and measurement using a zeroing neural dynamics approach," *Expert Syst. Appl.*, vol. 244, Jun. 2024, Art. no. 122938.
[30] T. Kim and T. Adalı, "Fully complex multi-layer perceptron network for nonlinear signal processing," *J. VLSI Signal Process. Syst. Signal Image Video Technol.*, vol. 32, pp. 29–43, Aug. 2002.
[31] A. Pande and V. Goel, "Complex-valued neural network in image recognition: A study on the effectiveness of radial basis function," *World Acad. Sci. Eng. Technol.*, vol. 1, no. 2, pp. 345–350, 2007.
[32] B. Liao, C. Hua, X. Cao, V. N. Katsikis, and S. Li, "Complex noise-resistant zeroing neural network for computing complex time-dependent Lyapunov equation," *Mathematics*, vol. 10, no. 15, p. 2817, Aug. 2022.
[33] L. Xiao, W. Huang, L. Jia, and X. Li, "Two discrete ZNN models for solving time-varying augmented complex Sylvester equation," *Neurocomputing*, vol. 487, pp. 280–288, May 2022.
[34] J. Jin, L. Zhao, L. Chen, and W. Chen, "A robust zeroing neural network and its applications to dynamic complex matrix equation solving and robotic manipulator trajectory tracking," *Frontiers Neurorobotics*, vol. 16, pp. 1–11, Nov. 2022.
[35] S. Li and Y. Li, "Nonlinearly activated neural network for solving time-varying complex Sylvester equation," *IEEE Trans. Cybern.*, vol. 44, no. 8, pp. 1397–1407, Aug. 2014.
[36] B. Liao, Q. Xiang, and S. Li, "Bounded Z-type neurodynamics with limited-time convergence and noise tolerance for calculating time-dependent Lyapunov equation," *Neurocomputing*, vol. 325, pp. 234–241, Jan. 2019.
[37] Y. Lei, J. Luo, T. Chen, L. Ding, B. Liao, G. Xia, and Z. Dai, "Nonlinearly activated IEZNN model for solving time-varying Sylvester equation," *IEEE Access*, vol. 10, pp. 121520–121530, 2022.
[38] L. Xiao and R. Lu, "A Finite-Time recurrent neural network for computing quadratic minimization with time-varying coefficients," *Chin. J. Electron.*, vol. 28, no. 2, pp. 253–258, Mar. 2019.
[39] L. Xiao, Y. He, Y. Li, and J. Dai, "Design and analysis of two nonlinear ZNN models for matrix LR and QR factorization with application to 3D moving target location," *IEEE Trans. Ind. Informat.*, vol. 19, no. 6, pp. 7424–7434, Jun. 2023.
[40] J. Jin, W. Chen, L. Qiu, J. Zhu, and H. Liu, "A noise tolerant parameter-variable zeroing neural network and its applications," *Math. Comput. Simul.*, vol. 207, pp. 482–498, May 2023.
[41] Y. Shtessel, C. Edwards, L. Fridman, and A. Levant, *Sliding Mode Control and Observation*. New York, NY, USA: Springer, 2014.
[42] P. Miao, Y. Shen, Y. Huang, and Y.-W. Wang, "Solving time-varying quadratic programs based on finite-time Zhang neural networks and their application to robot tracking," *Neural Comput. Appl.*, vol. 26, no. 3, pp. 693–703, Apr. 2015.

JIALIANG CHEN received the M.S. degree in systems analysis and integration from the School of Computer Science and Technology, Huazhong University of Science and Technology, Wuhan, China, in 2008.

He is currently with Jishou University. His research interests include neural networks and computer.

YIHUI LEI received the Ph.D. degree in statistics from Central South University, Changsha, China, in 2019.

She is currently an Associate Professor with the College of Mathematics and Statistics, Jishou University. Her research interests include neural networks, machine learning, and economic statistics.

BOLIN LIAO received the Ph.D. degree in communication and information systems from Sun Yat-sen University, Guangzhou, China, in 2015.

He is currently a Professor with the College of Computer Science and Engineering, Jishou University. He has published around 80 papers in various journals/conferences. His current research interests include neural networks, robotics, and nonlinear control.